J. Fluid Mech. (1965), *vol.* 22, *part* 4, *pp.* 709–720
Printed in Great Britain

The behaviour of freely falling cylinders and cones in a viscous fluid

By K. O. L. F. JAYAWEERA AND B. J. MASON
Physics Department, Imperial College, London

(Received 21 December 1964 and in revised form 15 March 1965)

The terminal velocities, drag coefficients, and orientations of single cylinders falling in a large tank of viscous liquid have been determined for Reynolds numbers *Re* ranging from $< 0{\cdot}01$ to 1000. Stationary eddies appear in the wakes of cylinders at $26 < Re < 50$, and the shedding of a Kármán vortex street at $Re > 50$ causes them to oscillate as they fall.

The interaction of two long, thin cylinders, which is largely determined by their initial relative positions, has been studied in some detail. One interesting result is that two equal cylinders, initially non-parallel and vertically separated by about 50 diameters, catch up and slide along each other until they bisect at right angles. When several cylinders are released in random orientations, they tend to cluster and then separate into pairs crossed at right angles and into triplets in the form of a symmetrical ++.

Cones with a flat base fall with apex upwards if the vertex angle $\theta < \frac{1}{4}\pi$ and with apex downwards if $\theta > \frac{1}{4}\pi$. Double cones, cemented base to base, and with apex angles θ_1 and θ_2 ($\theta_2 > \theta_1$), fall with acute apex upwards if $2\theta_1 + \theta_2 < \frac{3}{2}\pi$, the stable orientation being apex downwards if this condition is not satisfied. At $Re \simeq 100$, the shedding of a Kármán vortex street causes the cones to oscillate, while at $Re > 800$, the flow becomes highly turbulent and they tumble as they fall.

1. Behaviour of falling cylinders

The flow of a viscous fluid round an infinitely long circular cylinder has been studied theoretically by several workers, notably Bairstow, Cave & Lang (1923), Thom (1933), Tomotika & Aoi (1950), and Kawaguti (1953). The nature of the flow has also been studied experimentally, and drag coefficients have been measured for Reynolds numbers ranging from about $0{\cdot}5$ to $> 10^5$. The behaviour of freely falling cylinders at very low Reynolds numbers has been little studied, while the behaviour of small clusters of cylinders and needles is scarcely mentioned in the literature.

Gans (1911) showed that an ellipsoid of revolution at small Reynolds number would experience no resultant aerodynamic couple and hence could fall in any orientation. At larger Reynolds number, when the inertial forces become important, it may be shown (see Lamb 1932, pp. 174–7) that the ellipsoid will assume a stable orientation and fall along the direction of its shortest axis.

We may expect cylinders and needles to show much the same behaviour except in so far as the motion is affected by the flow at their ends.

In this study, small cylinders made either of Perspex, steel, or aluminium were allowed to fall through a large tank 30 cm × 30 cm × 80 cm deep containing either liquid paraffin, sugar solutions of different concentrations, or water, and were observed and photographed during their fall. With this combination of solids and liquids, it was possible to make careful observations on cylinders ranging in Reynolds number, defined as $Re = V_0 d/\nu$, where V_0 is the terminal velocity, d the cylinder diameter and ν the kinematic viscosity of the fluid, from $< 0{\cdot}01$ to about 100.

2. Terminal velocities and drag coefficients of cylinders

For a cylinder of length L and diameter d falling with its long axis horizontal at terminal velocity V through a viscous fluid, we may equate the net weight of the cylinder to the drag forces:

$$\tfrac{1}{4}\pi d^2 L(\rho_S - \rho_L) g = \tfrac{1}{2} C \rho_L V^2 dL \tag{1}$$

to give

$$C = \frac{\pi}{2}\frac{d}{V^2}\frac{(\rho_S - \rho_L) g}{\rho_L}, \tag{2}$$

where C is the drag coefficient, ρ_S, ρ_L are respectively the densities of the cylinder and of the fluid.

Lamb (pp. 614–16) derives the following relation between C and Re for a long, thin cylinder falling at low values of Re through an unbounded fluid

$$(C_\infty Re_\infty)_{d/L \to 0} = \frac{8\pi}{\frac{1}{2} - \gamma - \ln \frac{1}{8} Re_\infty}, \tag{3}$$

where γ = Euler's constant $= 0{\cdot}577$.

The effect of finite boundaries on the Stokes resistance of a particle has been investigated theoretically by Brenner (1962), who writes

$$F = \frac{F_\infty}{1 - k(F_\infty/6\pi\mu V D) + O(L/D)^3}, \tag{4a}$$

where F_∞ is the drag experienced by a particle falling in a long circular cylinder of diameter D, F is the drag when it is moving at the *same velocity* V in an unbounded fluid, and $k = 2{\cdot}1$.

Since from (1),

$$F_\infty = 4\pi\mu V_\infty L/(\tfrac{1}{2} - \gamma - \ln \tfrac{1}{8} Re_\infty),$$

equation (4a) may be re-written

$$F \simeq F_\infty \Big/ \left[1 - \frac{\frac{2}{3}k}{(\frac{1}{2} - y - \ln \frac{1}{8} Re_\infty)}\left(\frac{L}{D}\right)\right] = \frac{F_\infty}{\alpha}. \tag{4b}$$

If a cylinder falls at terminal velocity V_∞ in an infinite medium and at velocity V in a bounded medium of the same viscosity, the drag F is the same in both cases being equal to the effective weight. Thus

$$F = \tfrac{1}{2}\mu C_\infty Re_\infty V_\infty L = \tfrac{1}{2}\mu C Re V L, \tag{5}$$

where the subscripts refer to an infinite fluid, and

$$V_\infty/V = CRe/C_\infty Re_\infty. \tag{6}$$

If we denote by F_∞ the drag on a cylinder of the same length moving in an infinite fluid with velocity V, then C_∞ and Re_∞ take new values such that

$$F_\infty = \tfrac{1}{2}\mu C'_\infty Re'_\infty VL. \tag{7}$$

Using (5), (7) and (4*b*) we have

$$CRe/C'_\infty Re'_\infty = 1/\alpha. \tag{8}$$

Thus, from (6),

$$V_\infty/V = \frac{1}{\alpha}\frac{C'_\infty Re'_\infty}{C_\infty Re_\infty},$$

and since, for very small Re, (3) allows us to write $C'_\infty Re'_\infty \simeq C_\infty Re_\infty$,

$$V_\infty/V = Re_\infty/Re = 1/\alpha. \tag{9}$$

Substitution from (9) into (5) then gives

$$C_\infty/C = \alpha^2. \tag{10}$$

The present authors have determined the terminal velocities and drag coefficients of brass and steel needles falling through liquid paraffin, sugar solution, or water in a tank 30 cm × 30 cm × 80 cm deep. The terminal velocities of needles up to 8 cm in length and with $Re < 0{\cdot}2$ increase smoothly with increasing length to reach almost constant values as shown in figure 1.

We have used equations (9) and (10) to correct our experimental values of Re and C for the effects of the walls on our longest cylinders and so produce their corresponding values in an infinite fluid. These corrected values, given in table 1, also appear in figure 2 in which Lamb's formula, equation (3), is plotted for comparison. The agreement is quite close over the range $10^{-2} < Re < 0{\cdot}3$. Figure 2 also shows the results obtained by Finn (1953) and Tritton (1959), who measured the drag on cylindrical wires suspended in an air stream. The experimental values of the drag coefficients deviate progressively from Lamb's formula when Re increases beyond about 0·4. An alternative formula derived by Burgers (1938) and Broersma (1960) for the Stokes resistance of a long cylinder falling in an infinite fluid, viz.

$$\left.\begin{aligned} F_\infty &= 4\pi\mu LV_\infty/[\ln 2L/d + 0{\cdot}5 + O(d/L)^3], \\ \text{or}\qquad C_\infty Re_\infty &= 8\pi/[\ln 2L/d + 0{\cdot}5], \end{aligned}\right\} \tag{11}$$

gives much poorer agreement with the experimental results than does Lamb's formula for all values of $Re > 5\times 10^{-2}$. Indeed, equation (11) implies that, for a fixed value of L/d, $C_\infty Re_\infty = \text{const.}$, and experimentally this is certainly not the case.

The discrepancies are apparent in figure 1, where the experimental terminal velocities of cylinders falling in the tank are compared with values computed from both the Burgers–Broersma and the Lamb formula as corrected for wall effects by equation (4*b*). The agreement for long thin cylinders is good in all three cases at $Re = 0{\cdot}02$; at $Re = 0{\cdot}24$ the Burgers–Broersma formula gives velocities that are about 50 % too high.

As Re increases beyond unity, the effect of the walls becomes very small. Our experimental values of C and Re for $1 < Re < 10^3$ are plotted in figure 3 together with those of Relf (1913), Wieselsberger (1922) and Tritton (1959). The agreement

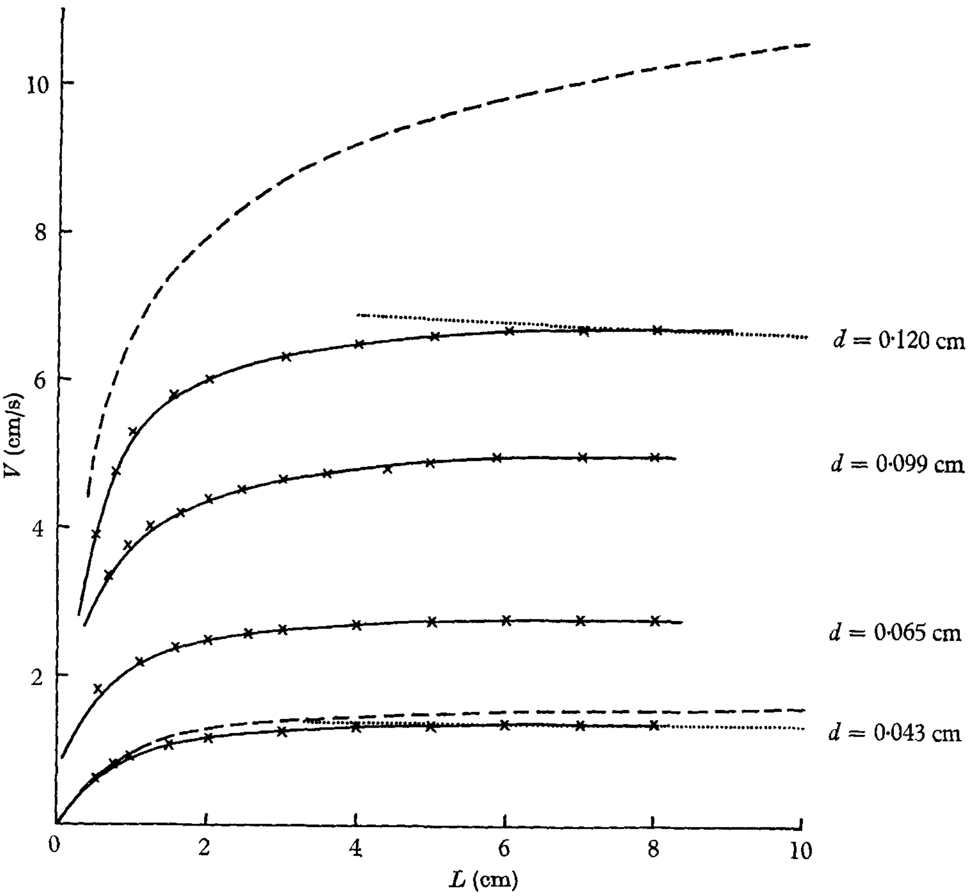

FIGURE 1. The terminal velocities of steel cylinders falling in liquid paraffin as functions of their length, L, and diameter, d. ×, experimental points; – – – –, Burgers-Broersma formula; · · · ·, Lamb.

Experimental		Corrected		
C	Re	C	Re	C Lamb's formula
34 ± 1	$0·24 \pm 0·01$	28·0	0·27	28·5
50 ± 1	$0·15 \pm 0·01$	43·5	0·16	43·0
85 ± 1	$0·075 \pm 0·005$	71·0	0·081	69·0
115 ± 3	$0·053 \pm 0·005$	97·0	0·055	95·0
195 ± 6	$0·028 \pm 0·002$	160·0	0·030	153·0
250 ± 8	$0·022 \pm 0·001$	200	0·023	195·0
280 ± 9	$0·0175 \pm 0·001$	236·0	0·019	225·0

TABLE 1. Measured and corrected values of C

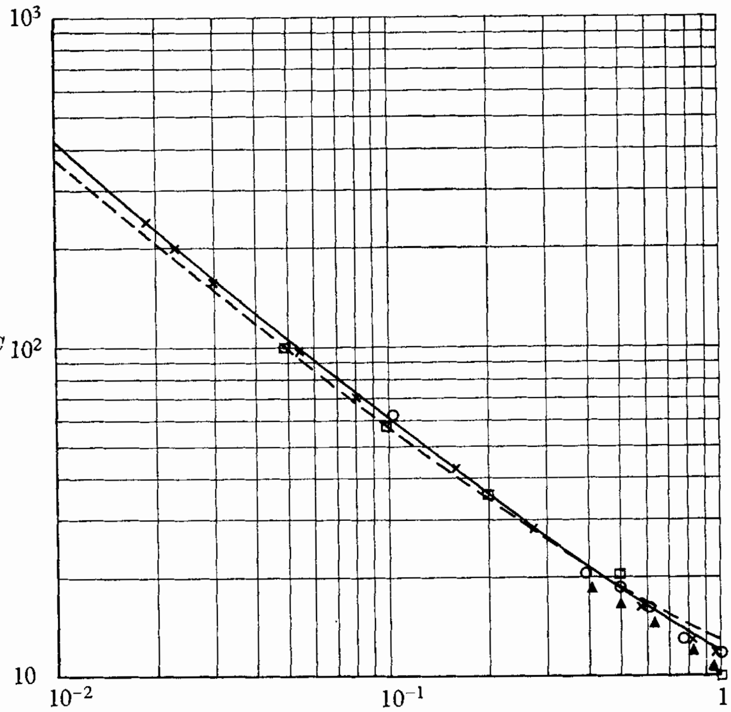

FIGURE 2. Drag coefficient C as a function of Reynolds number *Re* for long thin cylinders ($L/d > 100$) with $0{\cdot}01 < Re < 1$. ×, Our experimental values corrected for wall effects; ---, Lamb's formula; ▲, experimental values by Tritton; ○, Weiselsberger; □, Finn.

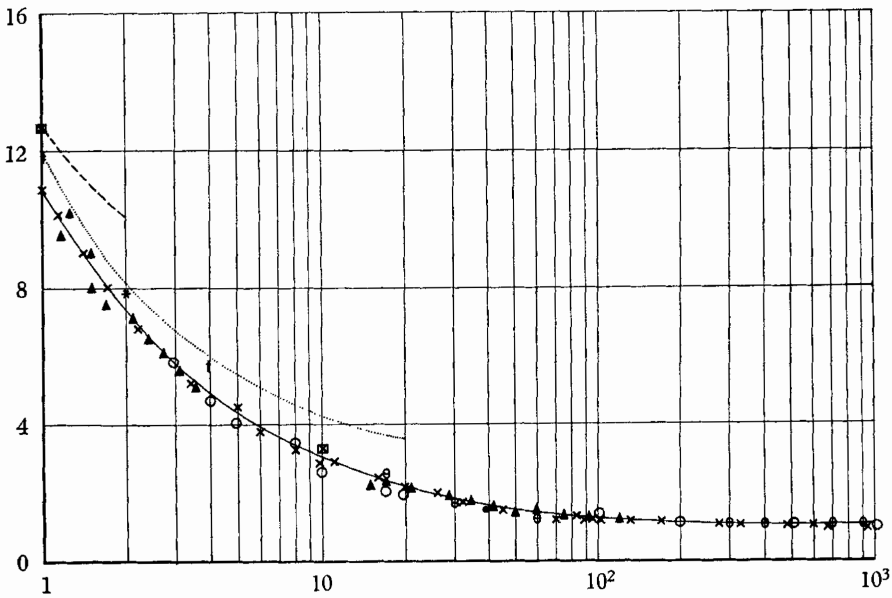

FIGURE 3. Drag coefficient C as a function of Reynolds number *Re* for long thin cylinders with $1 < Re < 10^3$. ×, Our experimental values; ▲ Tritton; ○, Weiselsberger; ⊖, Relf. ----, Lamb's formula; ····, formula of Bairstow *et al.*; ⊠, calculated values by Allen & Southwell; ●, Kawaguti; $*$, Southwell & Squire; †, Tomotika & Aoi.

between all these experimental data is quite impressive but they all give drag coefficients that are systematically lower than the theoretical values calculated by Bairstow *et al.* (1923), Thom (1933), Southwell & Squire (1934), Tomotika & Aoi (1950), Kawaguti (1953) and Allen & Southwell (1955).

3. Flow patterns, attitude and stability of falling cylinders

At very low Reynolds numbers, $Re < 0{\cdot}01$, the cylinders show no preferred orientation; they tend to fall in the same attitude with which they are released and with the direction of fall inclined to the vertical. However, for

$$0{\cdot}01 < Re < 0{\cdot}1,$$

the cylinders orient themselves to offer maximum resistance to motion so that those with $d/L > 1$ fall like disks with their short axis vertical; those with $d/L < 1$ fall with their long axis horizontal, and those with $d/L = 1$ fall in either orientation depending upon their attitude on release. At these low Reynolds numbers the cylinders oscillate before reaching their stable orientation but, when $Re > 0{\cdot}1$, the oscillations are heavily damped.

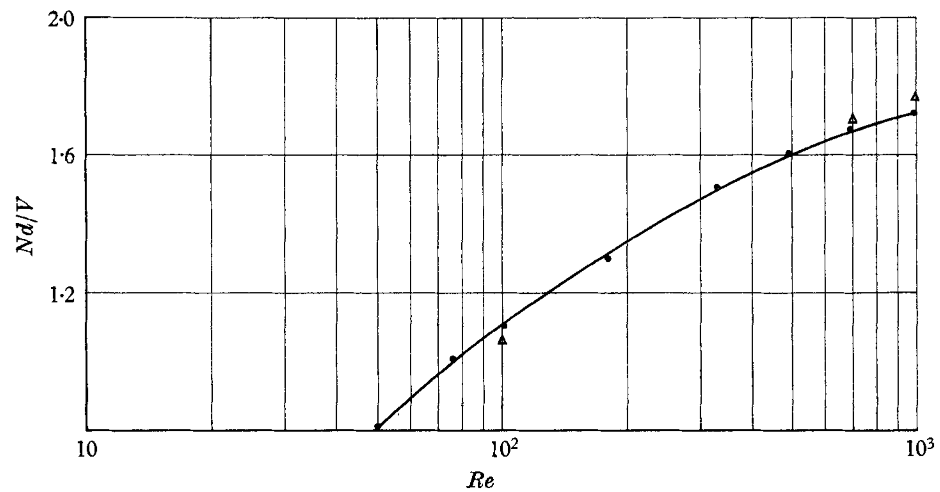

FIGURE 6. The rate of generation of eddies by falling cylinders of $Re > 50$ as a function of Reynolds number. ●, Our experimental values; △, values of Relf & Simmons.

The flow patterns behind the falling cylinders were revealed by coating them with water-soluble aniline dye and dropping them into a tank of sugar solution. As the Reynolds number increases beyond unity, the flow around the cylinder becomes increasingly asymmetric; the flow lines in the rear become reversed and give rise to two standing eddies of opposite rotation that first became distinct at $Re > 26$. In the case of short cylinders, flow past the ends give rise to a three-dimensional circulation which is pyramidal rather than cylindrical in shape, as shown in figure 4 (plate 1).

When Re exceeds 50, eddies separate from the surface of the cylinder and are shed as a Kármán vortex street. Vortices are shed regularly and alternately from opposite sides, and two sets of regularly spaced, expanding vortex rings of opposite rotation are formed along its trail as shown in figure 5 (plate 2). This observation is in agreement with that of Kovasznay (1949) who, using a hot-wire technique, detected periodic disturbances behind a cylinder at $Re > 40$. The frequency of eddy production N was measured and found to be dependent upon d, V_0 and Re. A plot of Nd/V_0 against Re gave a curve very similar to that obtained

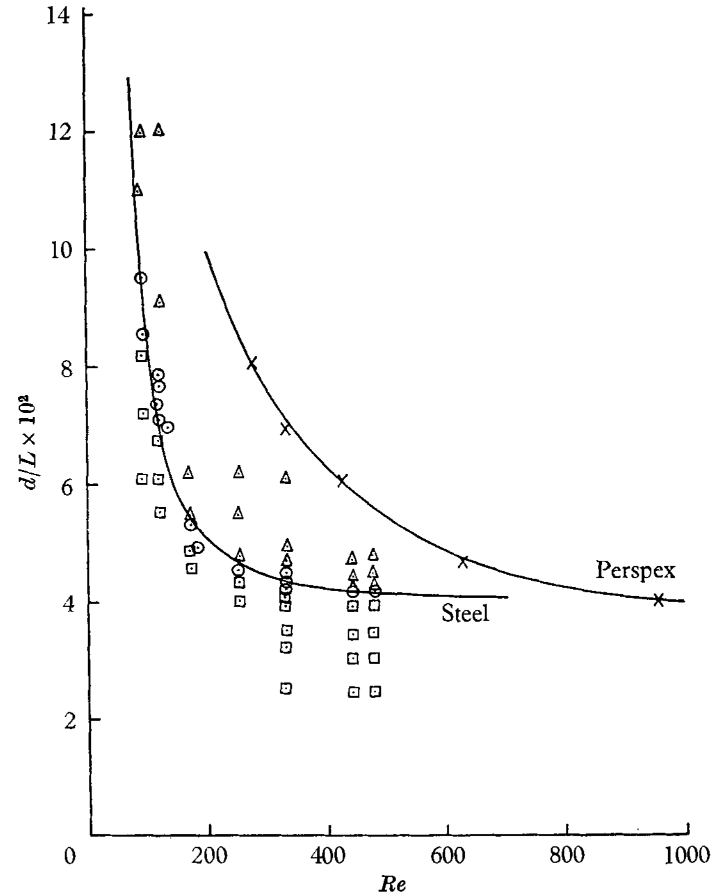

FIGURE 7. Observations on the transition from steady to fluttering motion of falling cylinders showing the influence of the d/L ratio and the Reynolds number. The curves indicate the transition between these two régimes for steel and Perspex cylinders. Individual observations are plotted only for steel as follows: ⊡, steady motion; ⊙, heavily damped oscillations; △, persistent fluttering.

by Relf & Simmons (1924) for ventilated stationary cylinders. Figures 3 and 6 show that, in this régime, the fall in drag coefficient with increasing Reynolds number is accompanied by a rise in the vortex frequency.

When eddies break away from the edges as well as the sides, the cylinder flutters about a horizontal axis through the centre and normal to its length. The amplitude of the oscillation is comparatively large for short cylinders, but decreases as the length increases, so that long cylinders fall stably. Although the transition from fluttering to steady fall is not abrupt, the observations of figure 7 allow a fairly definite boundary to be drawn between the two régimes. The critical value of d/L above which fluttering occurs decreases with increasing Reynolds number; for very short cylinders, the critical value of Re is about 50.

4. Behaviour of two equal falling cylinders

Two cylinders falling with $0{\cdot}1 < Re < 1$ were observed to interact when they were separated by as much as 100 cylinder diameters, and their behaviour was determined largely by their relative positions on being released into the tank of viscous liquid.

4.1. *Two long, thin, cylinders released simultaneously but separated horizontally*

(*a*) If the two cylinders are initially parallel, they rotate inwards and separate horizontally as they fall but still remain parallel to each other. In this respect they behave much like spheres (see Jayaweera, Mason & Slack 1964), in that the rates of rotation and separation decrease as the separation increases.

(*b*) If two cylinders are crossed on release, they slide relative to each other and attain a stable position in which they bisect each other at right angles. This stable configuration, which is achieved even when the initial angle of intersection is only 30°, is attained more rapidly at higher Reynolds numbers.

(*c*) Two cylinders separated horizontally but not parallel, flutter as they fall, but with decreasing amplitude, and eventually become parallel, and then separate as in (*a*) above. Simultaneous release is important in this experiment, otherwise the needles tend to become crossed.

(*d*) If two cylinders are released simultaneously in line but separated along their common axis, two distinct types of behaviour are observed. If $Re > 0{\cdot}1$, they continue to separate but preserve their initial orientation. If $Re < 0{\cdot}1$, the cylinders tilt in the vertical plane towards each other and flutter about a horizontal axis. The oscillations of both needles, which are 180° out of phase, gradually decrease, the needles eventually become parallel and then separate as in (*a*). This final position is attained more rapidly and with fewer oscillations at higher Reynolds numbers.

4.2. *Cylinders released with vertical separation*

(*a*) Cylinders released parallel and directly one behind the other:

When two identical, long, thin cylinders are released so that they fall parallel and close one behind the other, the trailing cylinder catches the leader, rotates round it, and when the line of centres becomes horizontal, they separate and fall as in §4.1 (*a*). Their velocity of approach, plotted as a function of separation, is shown in figure 8. Whereas for spheres the approach velocity decreases slowly to reach zero at large separations, with cylinders it drops sharply from a maximum value at a separation of about 30 diameters, to zero at about 80 diameters.

When the trailing cylinder is shorter and has a lower terminal velocity than the leader, it may catch the leader but only if the difference in terminal velocities is less than the maximum approach velocity for a pair of identical cylinders. In fact, measurements reveal that the relative motion of two unequal cylinders is equivalent to a linear superposition of their difference in terminal velocity upon the motion of two equal cylinders, the latter being controlled largely by the flow behind the leading cylinder.

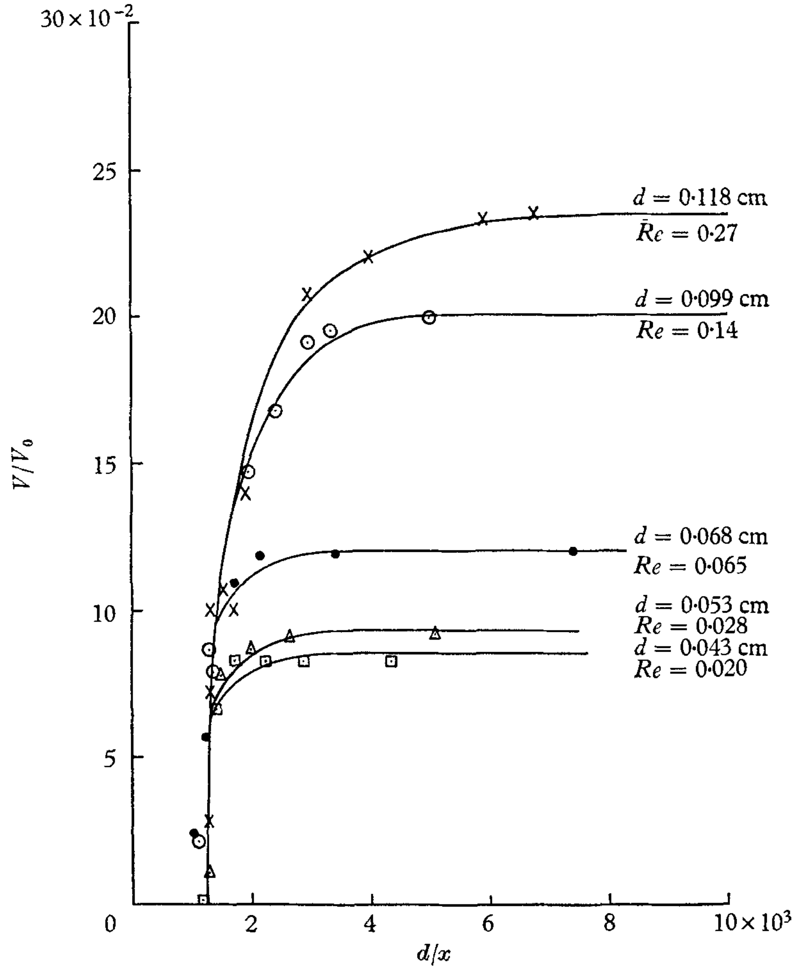

FIGURE 8. The velocity of approach of two equal, long, thin cylinders falling directly one behind the other as a function of their vertical separation x. V_0 is the terminal velocity of a single cylinder.

When the trailing cylinder is longer than the leader it tends to flutter as it overtakes the leader, but remains in the vertical plane common to both cylinders.

(*b*) Parallel cylinders displaced both horizontally and vertically:

The relative motion of such a pair of cylinders was determined by plotting their horizontal and vertical separation at successive intervals of time. The results are shown in figure 9. As the cylinders approach each other, they close more rapidly in the vertical than in the horizontal direction. At a certain stage, the horizontal separation remains sensibly constant while the vertical separation continues to decrease, but then it starts to increase again. Eventually the cylinders maintain a constant vertical separation and separate horizontally at a decreasing rate. In other words, two cylinders displaced horizontally are unable to catch up in either the vertical or horizontal planes, but follow a fixed path determined by their initial positions and then separate maintaining a fixed vertical separation.

(*c*) Cylinders not parallel:

The trailing cylinder tilts towards the leader and slides towards it. Both cylinders now flutter before taking up a stable position in which they bisect each other at right angles.

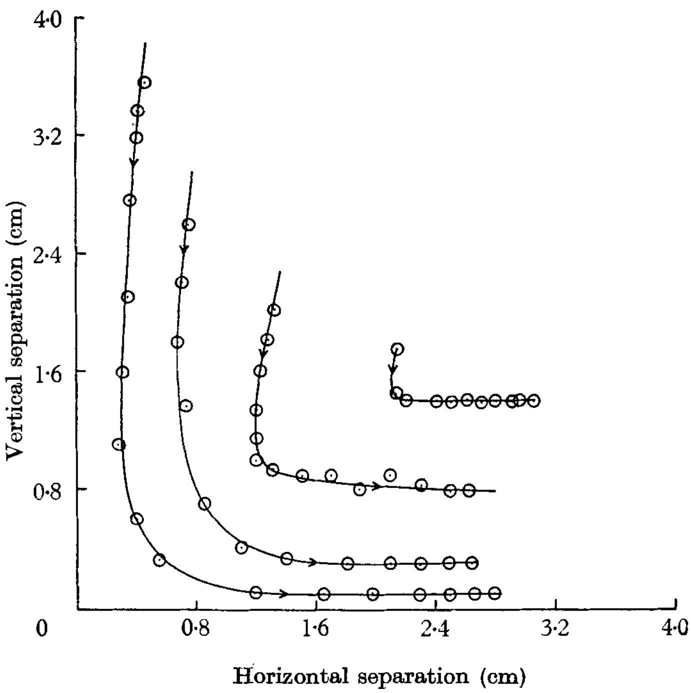

FIGURE 9. The relative motion of two equal long thin cylinders falling parallel to one another but separated in both the horizontal and vertical planes. Curves are drawn for different initial juxtapositions of the two cylinders and the points on a particular curve show the relative positions at $\frac{1}{4}$ sec intervals. The observations are for steel cylinders of $d = 0{\cdot}12$ cm, $L = 3$ cm falling in liquid paraffin.

5. Behaviour of three or more cylinders

When three or more identical cylinders are released simultaneously and parallel to one another, they continue to fall in the same horizontal plane but separate as they fall.

When several cylinders are released in random orientation, they may cluster to form symmetrical pairs crossed at right angles and also triplets in a symmetrical — pattern. While the crossed doublet is stable, the latter is not; the two parallel members separate, remaining parallel, while the upper cross member falls between and away from them. Two of these separating cylinders may later combine to form a symmetrical cross that falls faster than the remaining cylinder and leaves it behind.

6. Behaviour of falling cones

The behaviour of cones made of either Perspex or Duralloy was observed and photographed as they fell freely through a 30 cm-square tank containing either liquid paraffin or sugar solution at room temperature. The Reynolds numbers of the cones, defined in terms of the base diameter, ranged from 0·5 to 1500.

Cones having a flat base and $Re < 45$, fall with axis of symmetry vertical; if the apex angle θ is $< \frac{1}{4}\pi$, they fall steadily with apex pointing upwards, but, if $\theta > \frac{1}{4}\pi$, they fall apex downwards. Cones falling with apex upwards begin to flutter if Re exceeds about 45; those falling apex downwards and with

$$60^\circ < \theta < 80^\circ$$

are very steady at Reynolds numbers as high as 1500 and, even when $\theta > 80^\circ$, they do not flutter until Re exceeds 100.

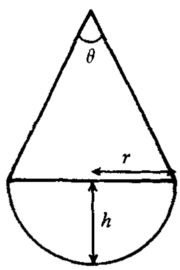

FIGURE 10.

Double cones, cemented base to base, with apex angles θ_1 and θ_2 ($\theta_2 > \theta_1$), also fall with axes vertical at Reynolds numbers less than about 200. For a given value of θ_2, the cone falls with the acute apex upwards if the angle θ_1 is less than a critical value, θ_1^*, given by

$$2\theta_1^* + \theta_2 = \tfrac{3}{2}\pi.$$

The cone achieves this final orientation whatever its initial orientation, even if it is released smoothly with the acute end pointing downwards. On the other hand, if $\theta_1 > \theta_1^*$, both orientations are possible, although if the cone suffers a small perturbation, it falls in its stable orientation with the acute angle θ_1 downwards.

Cones having a spherical cap, as shown in figure 10, were made to simulate falling hail pellets.

For a given value of the height h of the spherical cap, the particle falls with apex upwards if $\theta < \theta^*$ and with apex downwards if $\theta > \theta^*$, where

$$\theta^* = 0{\cdot}68h/r + \tfrac{1}{4}\pi.$$

This condition is observed to hold for values of h/r between 0·2 and 1·0.

The fluid flow around the falling cones was observed by coating them with soluble dye. At Reynolds numbers between about 5 and 200, depending upon the geometry and orientation of the cone, separation of the flow occurs at the circle of contact and standing eddies form in the wake of the cone as shown in figure 11 (plate 3). Above Reynolds numbers of about 50 for flat-based cones, and about 200 for hemispherically-capped cones, the eddies are shed alternatively from opposite sides of the cone which now begins to flutter (see figure 12, plate 4). At $Re > 800$, the flow becomes highly turbulent and erratic, and the cones tumble as they fall.

7. A note on falling disks

The authors have made a detailed study of the behaviour of falling disks for Reynolds numbers ranging from 0·07 to 600, but much of this work has been anticipated in a recent paper by Willmarth, Hawk & Harvey (1964). We confirm most of their observations on single disks and, in addition, have noted the interesting behaviour of two or more disks.

At $Re > 1$, attraction between two equal disks falling horizontally one directly behind the other is apparent at separations exceeding 40 diameters. As the rear disk is accelerated into the wake of the leader and closes to within 2 or 3 diameters, it begins to oscillate, and when the disks become very close they both oscillate together.

When the centres of the two disks are displaced by less than a radius, the rear disk catches up and comes to rest at an angle to the leader, which remains horizontal. At $Re > 100$, the angle between the two disks is $< 30^\circ$, but this inclination increases with decreasing Reynolds number and may approach 90° at $Re \simeq 5$.

A cluster of three equal disks forms a 'butterfly' configuration in which one member remains horizontal and the other two form a symmetrical vee in its rear. Such a cluster is very stable when the angle $\theta < 30^\circ$, and falls without fluttering; only at high Reynolds numbers, when the flow becomes highly turbulent, does it tend to break up.

REFERENCES

Allen, D. N. de G. & Southwell, R. V. 1955 *Quart. J. Mech. Appl. Math.* **8**, 129.
Bairstow, L., Cave, B. M. & Lang, E. D. 1923 *Phil. Trans.* A, **223**, 383.
Brenner, H. 1962 *J. Fluid Mech.* **12**, 35.
Broersma, S. 1960 *J. Chem. Phys.* **32**, 1632.
Burgers, J. M. 1938 *Kon. Ned. Akad. Wet. Verhand* (Eersti Sectie), D1, **16**, 1.
Finn, R. K. 1953 *J. Appl. Phys.* **24**, 771.
Gans, R. 1911 *Sitzber. Akad. München*, **41**, 197.
Jayaweera, K. O. L. F., Mason, B. J. & Slack, H. W. 1964 *J. Fluid Mech.* **20**, 121.
Kawaguti, M. 1953 *J. Phys. Soc. Japan*, **8**, 474.
Kovasznay, L. S. G. 1949 *Proc. Roy. Soc.* A, **198**, 174.
Lamb, H. 1932 *Hydrodynamics*, 6th ed. Cambridge University Press.
Relf, E. F. 1913 *Tech. Rep. and Memo. Adv. Comm. Aero* (*A.R.C.*), London, no. 102.
Relf, E. F. & Simmons, L. F. G. 1924 *ARC Rep. and Mem.* no. 917.
Southwell, R. V. & Squire, H. B. 1934 *Phil. Trans.* A, **232**, 27.
Thom, A. 1933 *Proc. Roy. Soc.* A, **141**, 651.
Tomotika, S. & Aoi, T. 1950 *Quart. J. Mech. Appl. Math.* **3**, 140.
Tritton, D. J. 1950 *J. Fluid Mech.* **6**, 577.
Wieselsberger, C. 1922 *Phys. Z.* **22**, 321.
Willmarth, W. W., Hawk, E. & Harvey, R. L. 1963 *Phys. Fluids*, **7**, 197.

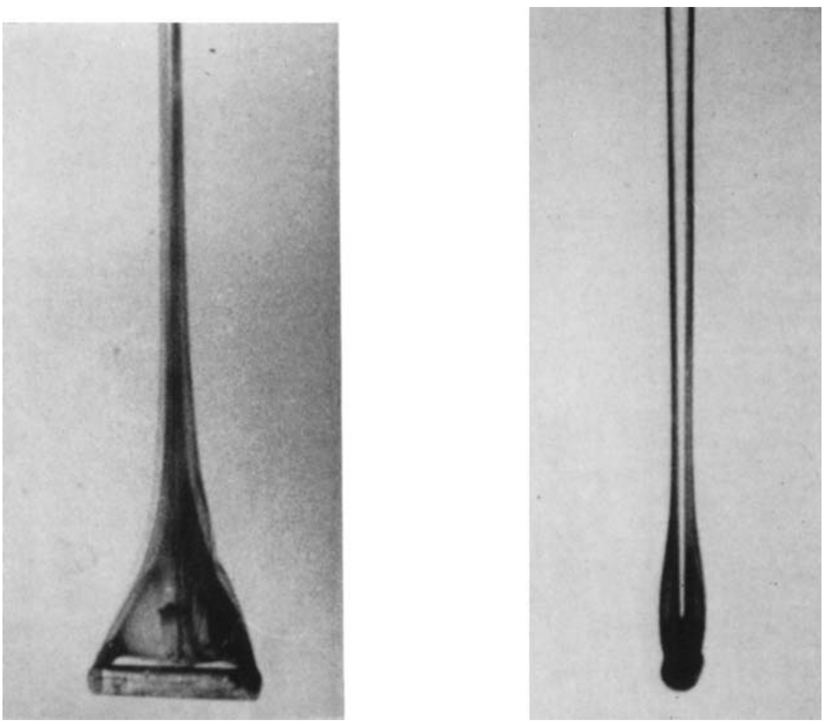

(*a*) (*b*)

FIGURE 4. Closed eddies formed behind a short falling cylinder of $Re = 40$. (*a*) Broadside-on, (*b*) end-on.

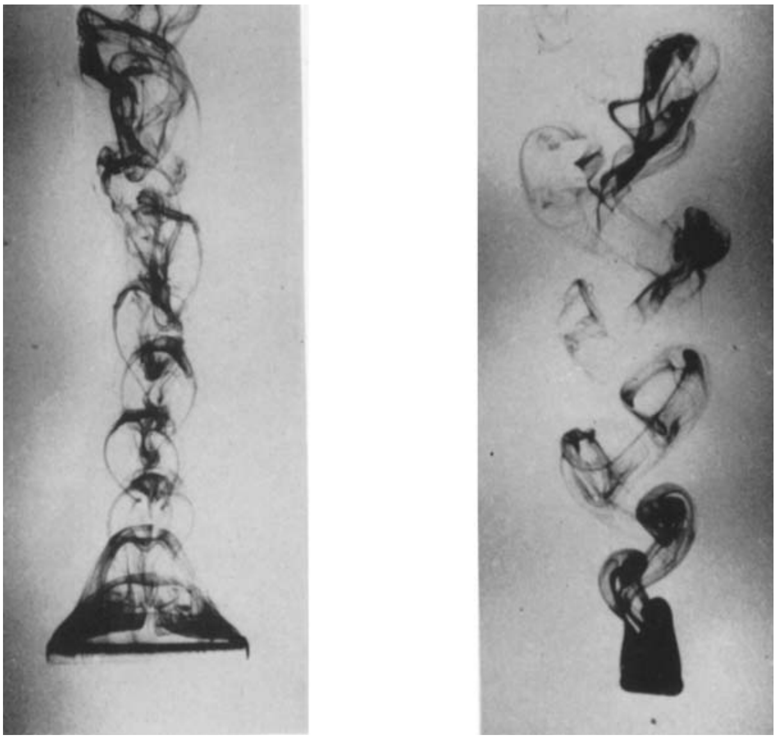

(*a*) (*b*)

FIGURE 5. Shedding of vortices by a falling cylinder of $Re = 70$. (*a*) Broadside-on, (*b*) end-on.

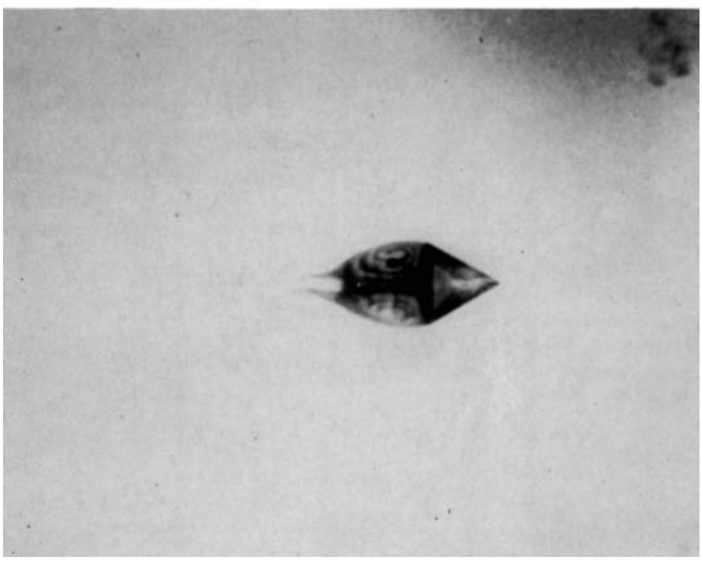

(*a*)

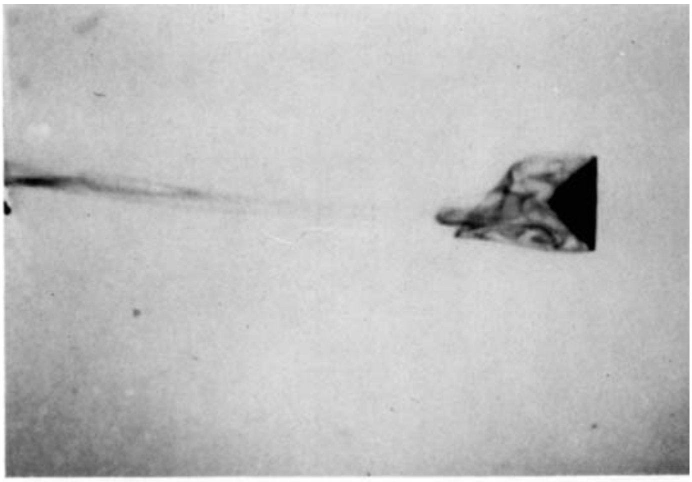

(*b*)

FIGURE 11. Closed eddies formed in the wakes of flat-based cones with $Re = 17$. (*a*) Cone falling with apex downwards, (*b*) with apex upwards.

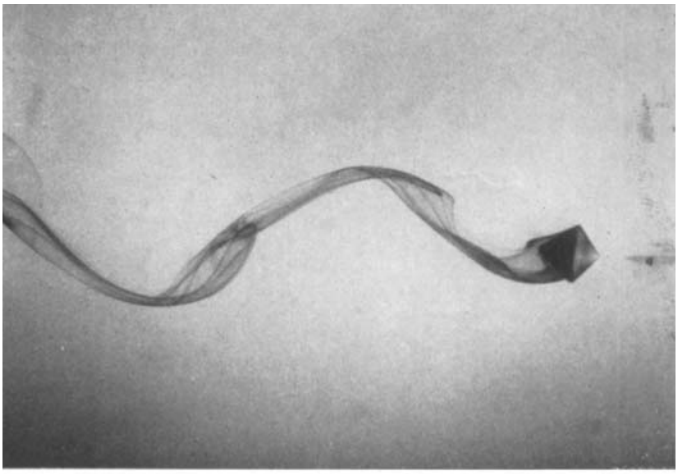

(*b*)

(*a*)

FIGURE 12. Shedding of eddies by cones of $Re = 230$ which flutter as they fall. (*a*) Cone with spherical cap, (*b*) double cone.